Iranian Reasearch Organization
for Science and Technology
(IROST)

Advances in Environmental Technology 11(3) 2025, 329-340.

Advances in Environmental Technology

Journal home page: https://aet.irost.ir

Cu removal from wastewater using a polyethersulfone- graphene oxide nanoparticles functionalized with chitosan membrane

Iman Khonsha*[a], **Kobra Salehi**[b]

[a] *Department of Chemical Engineering, Shiraz Branch, Islamic Azad University, Shiraz, Iran.*

[b] *Department of Chemical Engineering, Darab Branch, Islamic Azad University, Darab, Iran.*

ARTICLE INFO

Document Type:
Research Paper

Article history:
Received 24 November 2024
Received in revised form
16 April 2025
Accepted 29 April 2025

Keywords:
Graphene Oxide GO
Chitosan
Polyethersulfone (PES)
membrane
Mixed matrix membrane

ABSTRACT

In this study, graphene oxide (GO) nanoparticles were synthesized from a graphite precursor using a simplified Hummer method, and their surfaces were functionalized with chitosan to improve their dispersion and compatibility with the polymer matrix. The functionalized nanoparticles were then incorporated into polyethersulphone (PES) membranes to enhance their properties and provide mixed-matrix membranes. For the fabrication of the polyethersulfone membranes and their performance, an experimental design was performed using Minitab 17 software, applying the Taguchi method with an L9 orthogonal array. The parameters influencing membrane performance, including the polymer and GO concentrations in the membrane casting solution and operating pressure during the separation process, were selected at three levels. The results showed that increasing the polymer concentration enhanced Cu removal but reduced the permeate flux, whereas higher pressure increased the flux but decreased the separation efficiency. In addition, contour plots representing the permeate flux and Cu removal% as a function of the polymer concentration and the operating pressure indicated that the maximum Cu removal (> 70 wt. %) occurred within the pressure range of 6 to 6.2 bar and polymer concentration of 18 to 20 wt.% in the casting solution.

1. Introduction

Industrial wastewater contains various organic and inorganic pollutants. Among them, heavy metals can be toxic and carcinogenic, and some can create poisonous compounds even at very low concentrations [1-3]. One of the biggest challenges with environmental heavy metal pollution is the difficulty in removing heavy metals from wastewater because of their high mobility and nonbiodegradability [4, 5]. Copper is an essential heavy metal, and its compounds are widely used in various industries [6-9], with concentrations of up to 500 ppm [8]. However, the EPA allows a maximum of 1.3 ppm of copper in industrial wastewater [10, 11]. Conventional methods for organic compound removal cannot eliminate metals because metal removal requires altering

---

*Corresponding author Tel.: +98 9173375697
E-mail: iman.khonsha@iau.ac.ir

DOI: 10.22104/AET.2025.7217.1987

their chemical states through specific processes [3]. Various physicochemical methods, like adsorption and ion exchange, have been proposed for heavy metal removal; however, many of these methods face economic and technical challenges [12-15]. Recently, membrane technology has become popular because of its ease of use [16, 17]. This modern system effectively eliminates heavy metals using techniques such as reverse osmosis and ultrafiltration [14, 18]. Mixed-matrix membrane separation also has widespread applications in various fields, particularly water and wastewater treatment, due to its effective purification and economic, social, and environmental benefits [19, 20]. Numerous research efforts have investigated the use of membrane filtration techniques to remove heavy metal ions [21-26]. Hasan and Hassoon used polytetrafluoroethylene hydrophobic (PTFE) and acrylic copolymer (HCP) to remove Cu ions from wastewater [27]. Nawaz et al. comprehensively investigated the extraction of Cu ions using a tri-ethanolamine/cyclohexanone-based supported liquid membrane (SLM) [28]. Yang et al. developed a detailed mechanism for Cu-ion transport from ammoniacal wastewater using a hollow fiber-supported liquid membrane (HFSLM) system [29]. Bouguerra et al. investigated the use of supported liquid and polymer inclusion membranes (PIMs) for Cu transport in a continuous extraction-re-extraction system [30]. Akale and Shaikh comprehensively examined the permeability and separation capabilities of polysulfone mixed matrix membranes with Al_2SiO_6 powder [31].

Khodabakhshi and Goodarzi fabricated an innovative ternary mixed matrix membrane based on polyethersulfone/sulfonated polyethersulfone/organically modified nanoclay and studied its ability to remove heavy metals from wastewater [32]. Nasr et al. successfully fabricated mixed matrix forward osmosis membranes using polyethersulfone and GO nanosheets and evaluated their performance for water desalination applications [33]. Polyethersulfone is a widely used commercial polymer exhibiting high mechanical and thermal stability, resistance to heat aging, environmental durability, and ease of processing [34]. However, the hydrophobic nature of PES results in low membrane flux and significant fouling problems [35]. Physical or chemical modifications are required to enhance the hydrophilicity of PES membranes. GO, as a promising carbon-based material, offers a large surface area, excellent mechanical strength, and outstanding hydrophilicity, making it an ideal candidate for modifying polymeric membranes [36, 37]. The exceptional hydrophilicity of GO is attributed to the presence of various oxygen-containing functional groups on its surface: hydroxyl, epoxide, carbonyl, and carboxyl groups. According to published research, functionalizing GO can also significantly enhance its selectivity for adsorption, increase its adsorption capacity, especially for various heavy metal ions, and facilitate the separation of spent GO from water [38-39]. This study focuses on fabricating polyethersulfone membranes and mixed-matrix membranes using synthesized GO nanoparticles functionalized with chitosan and investigating their performance in Cu removal from wastewater. This study presents a novel approach to Cu removal from wastewater using polyethersulfone-GO nanoparticles functionalized with a chitosan membrane. To our knowledge, this is the first time such a membrane has been synthesized and evaluated for this specific purpose.

2. Experimental Work

2.1. Materials

The polyethersulfone with a molecular weight of 58,000 Daltons was obtained from BASF, Germany. The N, N-dimethylacetamide (DMA) and copper (II) chloride dehydrate were procured from Merck, Germany, and the chitosan with a medium molecular weight from Sigma-Aldrich, USA. The sulfuric acid (purity ≥ 98%), potassium permanganate (high purity), and graphite (fine powder extra pure) used to produce the membrane were acquired from Merck, Germany. All chemical substances were used in their received form without any additional purification processes. Additional equipment used included an oven, digital scale, ultrasonic bath, magnetic stirrer, membrane film-casting rod, coagulation bath, other auxiliary equipment for membrane manufacturing, and a module device for evaluating membrane performance.

2.2. Method

2.2.1. Preparation of Chitosan-Modified Graphene Oxide Nanoparticles

To synthesize the GO using a simplified Hummer method, 2 g of pure graphite was added to 46 ml of 98% sulfuric acid and placed in an ice bath maintained at a temperature below 10°C. After stirring for 15 min, 6 g of potassium permanganate was slowly introduced into the mixture under high-speed stirring, which was continued for 7 h. The agitation process was sustained for an extended duration of 30 min. The temperature of the bath was then increased to 35°C, and the mixture was stirred for 1 h. To dilute the mixture, 400 ml of distilled water was gradually added while stirring for 30 min. Subsequently, 20 ml of 30% hydrogen peroxide was slowly added, and mixing was continued for another 30 min, during which the solution briefly turned bright yellow. To remove ions and increase the pH, the mixture was washed with 10% hydrochloric acid and distilled water, stirred for one hour, and then left to stand for approximately four hours. The resulting solid product, graphene oxide, was separated from the liquid phase by filtration. The GO was then dried in an oven at 50°C for 2 h. Next, the dried GO was placed in an ultrasonic bath with 2 ml of ethanol for 1 h. Then, 0.3 mg of the prepared chitosan nanoparticles were added to this solution, and the mixture was stirred for 20 h. The product was washed and dried at 80°C for 16 h [40-42] .

2.2.2 Experimental Design by the Taguchi Method

For the PES membrane fabrication, an experimental design was performed using Minitab 17 software, applying the Taguchi method with an L9 orthogonal array. Three key parameters influencing membrane separation, including the polymer and GO percentages in the membrane casting solution and the operating pressure during separation, were selected at three levels: a) 15%, 18%, and 21% for polymer percentage; b) 0%, 0.3%, and 0.7% for nanoparticle percentage; and c) 6, 8, and 10 bar for operating pressure. The experimental design results are presented in Table 1.

Table 1. Results of the experimental design using the Taguchi method.

Experiment No.	Polymer wt.%	Graphene wt.%	Pressure (bar)
1	15	0	6
2	15	0.3	8
3	15	0.7	10
4	18	0	8
5	18	0.3	10
6	18	0.7	6
7	21	0	10
8	21	0.3	6
9	21	0.7	8

According to Table 1, membrane solutions, including three pure polymer solutions and six polymer solutions containing GO NPs, were prepared using the following method [42].

2.2.3. Membrane Fabrication

Polyethersulfone was first dried at 80°C for 4 h to fabricate the mixed-matrix membrane. To prepare solutions without GO, the polymer was added to DMA and stirred for 24 h with heating. In the case of GO-containing solutions, the GO was first added to the solvent and placed in an ultrasonic bath for 10 min to ensure the complete dispersion of the nanoparticles. Afterward, polyethersulfone was added to the suspension, stirred for 24 h using a magnetic stirrer, and left for 24 h to remove any bubbles from the solution [42].

To enhance the mechanical strength of the membrane, a polyester sheet was used as a support on a glass, with four layers of adhesive applied around it, to achieve the desired thickness. The polymer solution was then poured on this support, and a filming device was uniformly drawn across the polymer solution at a constant speed. Immediately after film formation, the membrane was transferred to a coagulation bath containing distilled water (non-solvent bath). Once the membrane had been created and separated from the glass, it was placed in a distilled water bath for 24 h to remove the solvent from its structure. The membrane was then dried in an oven at 100°C.

2.2.4. Membrane Evaluation Methods

The morphologies, pore sizes, and effects of the GO nanoparticles on the membrane structure were investigated to evaluate the performance of the fabricated membranes. For this purpose, the surface morphologies of the membranes were analyzed using scanning electron microscopy (SEM). The membrane sheets were placed in a module, and a reverse-osmosis membrane system consisting of a feed tank, pump, control valve, flowmeter (1), pressure gauge, membrane module, and flowmeter (2) was then assembled for this purpose, as seen in Figure 1.

A feed solution containing 150 ppm of Cu ions was passed through the membrane system under the experimental design conditions. Samples were diluted with deionized water to Cu concentrations ranging from 0.05 to 5 ppm. Copper ion concentrations were then measured using atomic absorption spectrometry at a wavelength of 324.7 angstroms, according to ASTM D1688. The Cu removal efficiency was calculated by measuring the concentration of Cu ions in the permeate using an atomic absorption device.

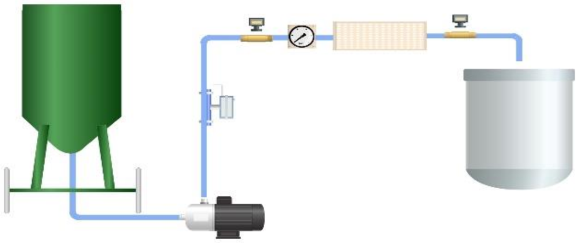

Fig.1. Reverse osmosis setup used for Cu separation from water by the membrane.

2.2.5. Statistical Analysis

The Design of Experiments (DOE) approach was conducted using Minitab software (Version 17) to plan and analyze the experiments systematically. The collected data were evaluated for normality and homogeneity of variance.

Analysis of variance (ANOVA) was performed to determine the significance of the experimental factors and their interactions. The p-values were assessed at a confidence level of 95% ($\alpha = 0.05$) to identify statistically significant effects. Additionally, R^2 and adjusted R^2 values were examined to assess the goodness of fit of the statistical model.

All statistical and graphical analyses were performed using Minitab, ensuring reliable interpretation of the experimental data.

3. Results and Discussion

3.1. Morphology of Prepared Membranes

The SEM images showed that the membrane consisted of an upper, middle, and bottom layer. The upper layer was dense and relatively smooth, with a few voids where filtration occurred. The middle layer featured a finger-like structure that supported the upper filtration layer and the bottom layer. Some walls in the middle layer contained micro-holes, while others were relatively smooth and solid. The solution containing heavy metals penetrated the outer surface and became trapped within the membrane pores, effectively preventing the passage of heavy metal compounds through the membrane. The presence and uniform dispersion of nanoparticles within the pores and membrane matrix resulted in smaller pore sizes. This modification enhanced the membrane's ability to block heavy metal molecules, thereby improving the separation efficiency. However, the introduction of nanoparticles also led to a reduction in flux compared with membranes made from pure polymers. Figure 2a, b show cross-sectional SEM images of membranes prepared from a casting solution containing 18 wt.% polyethersulfone, without and with 0.7 wt.% GO nanoparticles, respectively.

3.2. Investigating Membrane Performance

The membrane performance was systematically examined using an experimental framework predicated on the Taguchi methodology. The parameters of operation were comprised of polymer concentration levels (15%, 18%, 21%), concentrations of GO nanoparticles (0.0%, 0.3%, 0.7%), and applied operational pressures (6, 8, 10 bar), each evaluated at three distinct levels. The experimental trials were executed to evaluate the percentage of Cu removal, which was ascertained by comparing the initial concentration of Cu ions in the feed solution with that in the permeate, using an atomic absorption spectrophotometer. The findings are summarized in Table 2. Agitation was sustained for an additional 30 minutes. All reagents were used as received without further purification. For scrutinizing the experimental outcomes, statistical methodologies alongside outputs derived from Minitab software were employed to analyze variance (ANOVA). The influences of polymer concentration, GO nanoparticle concentration, and operational pressure on the membrane efficacy during the separation of Cu ions from aqueous solutions were systematically investigated. The R-squared (R-sq.) and adjusted R-squared (R-sq. (adj)) metrics are delineated in Table 3, and the corresponding p-values are elucidated in Table 4. The R-squared value of 91.09% indicated that the statistical model conformed to the experimental data and effectively elucidated the outcomes. The adjusted R-squared value (R-sq(adj)) of 85.75% demonstrated that despite the complexity of the model, the results were sufficiently elucidated. Furthermore, according to the regression results delineated in Table 4, the polymer and GO concentrations and operating pressure were identified as the principal factors affecting the membrane performance in Cu removal. The p-values of 0.011, 007, and 0.01 for the polymer concentration, GO concentration, and operating pressure indicated a statistically significant impact on the membrane performance with a high degree of confidence. The analysis of variance for water permeate flux through the membrane is shown in Table 5, 6.

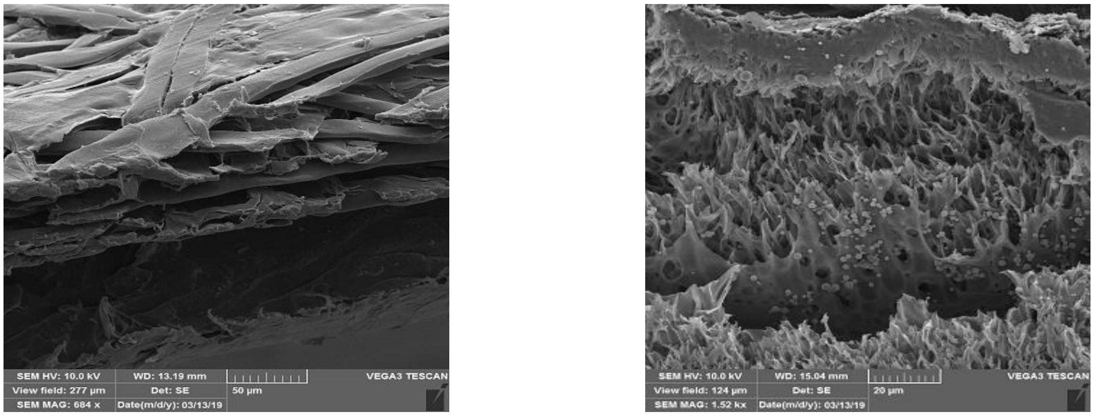

(a) (b)

Fig. 2. Cross-sectional SEM images of membranes prepared from a casting solution containing 18 wt.% polyethersulfone a) without GO nanoparticles and b) with 0.7 wt.% GO nanoparticles.

Table 2. Results of Cu removal and fluid flux under the experimental design conditions.

Exp. No.	Polymer wt.%	GO wt.%	Pressure (bar)	Cu removal wt.%	Flux through mem. (L/hr.m^2)
1	15	0	6	58.2	216.5
2	15	0.3	8	59.3	237
3	15	0.7	10	60.1	244
4	18	0	8	61	220
5	18	0.3	10	59.3	247
6	18	0.7	6	70.5	176
7	21	0	10	60	200
8	21	0.3	6	67.1	145
9	21	0.7	8	66.2	168

Table 3. Model summary for Cu removal%.

S	R-Sq	R- Sq(adj)
2.6592	91.09%	85.75%

Table 4. Analysis of variance for Cu removal%.

Source	DF	Adj SS	Adj MS	F-Value	P-Value
Regression	3	138.47	46.157		0.005
Polymer%	1	41.08	41.082	20.07	0.011
GO%	1	52.56	52.562	5.00	0.007
P	1	44.83	44.827	15.87	0.01
Residual Error	5	13.54	2.708		
Total	8	152.01			

Table 5. Model summary for water permeate flux.

S	R-Sq	R- Sq(adj)
9.77114	95.45%	92.72%

Table 6. Analysis of variance for water permeate flux through membrane.

Source	DF	Adj SS	Adj MS	F-Value	P-Value
Regression	3	10015.8	3338.62	34.97	0.001
Polymer%	1	5673.4	5673.37	59.42	0.001
GO%	1	415.4	415.43	4.35	0.091
P	1	3927,0	3927.04	41.13	0.001
Residual Error	5	477.4	95.48		
Total	8	10493.2			

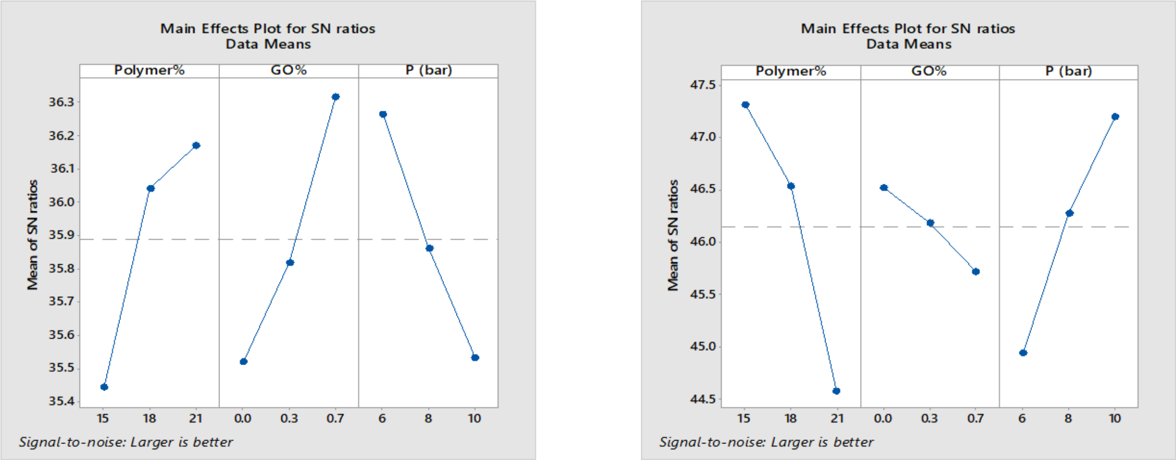

(a) (b)

Fig. 3. Main effects plot for the signal-to-noise (S/N) ratio related to a) the Cu removal% from water by membrane and b) the water permeate flux.

The R-squared value of 95.45% signified that the statistical model conformed to the experimental data. Furthermore, the polymer and operating pressure had a highly significant effect on water permeate flux, whereas the GO concentration was not statistically significant at the 0.05 level ($p > 0.05$).

Figure 3a, b illustrate the main effects plots for the signal-to-noise (S/N) Ratios for Cu removal% and water permeate flux, depicting the effect of each parameter on membrane performance. The signal-to-noise ratio followed the "Larger is Better" criterion, indicating that higher values corresponded to more effective copper removal.

The pronounced positive gradient observed in the polymer and GO concentration graphs implied that fluctuations in polymer and GO concentrations exerted a substantial influence on the signal-to-noise (S/N) ratio in Cu removal, hence indicating that an increase in polymer or GO concentration correlated with improved membrane efficacy. In contrast, the observed negative gradient in the signal-to-noise (S/N) ratio graph as a function of pressure suggested that an elevation in pressure resulted in a corresponding decline in the S/N ratio; stated differently, an increase in operational pressure engendered adverse repercussions on the performance of the system. This phenomenon might be attributed to excessive pressure, which could induce heightened noise or instability within the process, ultimately compromising the efficacy of the membrane in the separation of copper ions. These results aligned with previously examined p-values.

The pronounced negative gradient in the polymer concentration and positive gradient in the pressure graphs implied that fluctuations in polymer concentration and pressure exerted a substantial influence on the signal-to-noise (S/N) ratio in the water permeate flux. The negative and relatively gentle gradient of the GO nanoparticle concentration graph indicated that the proportion of nanoparticles did not exert a notable impact on the S/N ratio in water flux.

Figure 4a, b delineate the main effects plot for means related to Cu removal and water permeate flux, which encapsulated the average influence of each parameter on the permeate flux across the membrane.

As evidenced by the findings, there exists a concordance within the confidence intervals pertaining to the polymer concentrations of 15% and 18%, as well as across all three levels of GO concentrations and applied pressures within the Cu removal representations. This concordance implies that no statistically significant distinctions are present among these levels.

In the water permeate graphs, the pronounced negative gradient observed in the polymer concentration indicated that the mean permeate flux experienced a substantial decline as polymer concentration increased. This phenomenon implied that elevated polymer concentrations promoted a more compact membrane architecture characterized by reduced pore dimensions, consequently impeding permeation through the membrane. The mild negative gradient associated with the GO nanoparticle concentration implied that the GO nanoparticles exerted a negligible detrimental influence on the mean permeate flux. This observation might be attributable to the relatively low proportion of nanoparticles, which were unlikely to cause significant modifications to the membrane architecture. In contrast, the pronounced positive gradient associated with the operating pressure signified that an increase in the operating pressure considerably enhanced the permeate flux. This phenomenon was expected as elevated pressure intensified the driving force across the membrane, thereby augmenting the flow efficiency. Figure 5a, b, c and Figure 6a, b, c show the interval plots for Cu removal and water permeate flux.

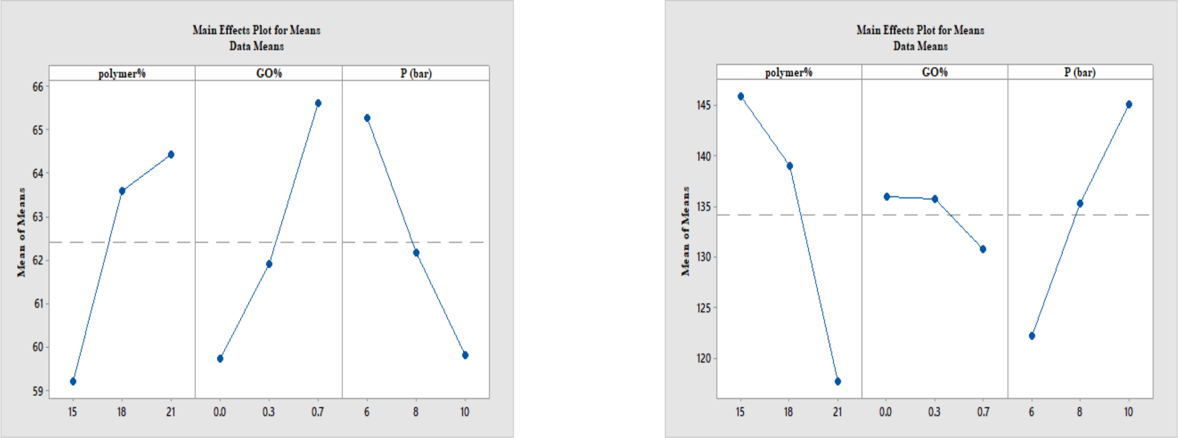

(a) (b)

Fig. 4. Main effects plot for Means for a) Cu removal% and b) water permeate flux through membrane

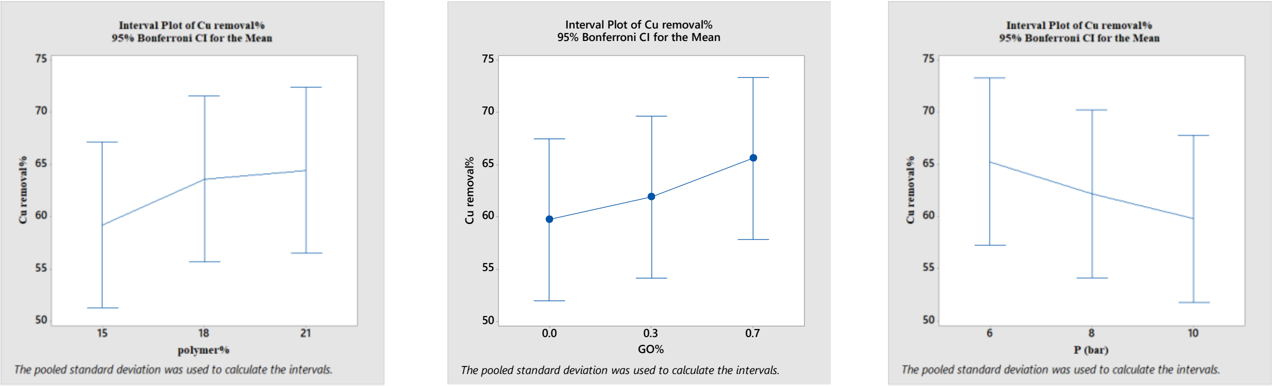

(a) (b) (c)

Fig. 5. The interval plots for Cu removal percentage as a function of a) polymer concentration, b) GO concentration, and c) process pressure

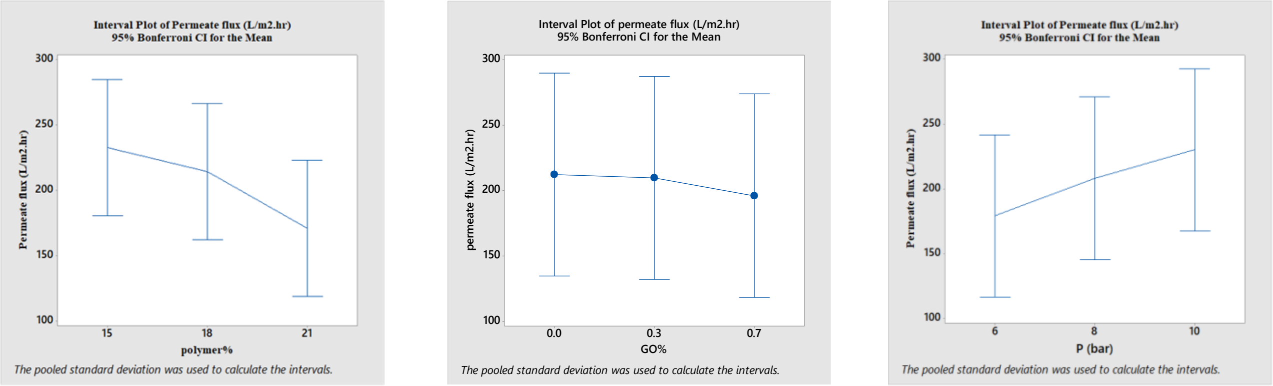

(a) (b) (c)

Fig. 6. The interval plots for permeate flux as a function of a) polymer concentration, b) GO concentration, and c) process pressure.

The interval plots for Cu removal and permeate flux show the following:

1) As the polymer concentration increased, the mean Cu removal efficiency increased up to a certain point. Beyond the optimal range, the intervals slightly overlapped, indicating a diminishing effect at high concentrations. This result was consistent with the regression results, in which the polymer concentration had a positive but moderate effect. The highest flux was observed at a polymer concentration of 15%, whereas increasing the polymer concentration to 21% resulted in a decrease in flux due to an increase in the membrane structure density and a decrease in its porosity and permeability.

2) There was an upward trend in the GO nanoparticle concentration, and higher GO content led to significantly improved Cu removal. However, very high GO concentrations might cause aggregation, thereby reducing the effectiveness. The addition of different amounts of GO nanoparticles did not significantly change the flux. This could be due to the low amount of GO used. In some studies, increasing GO up to a certain level could improve membrane performance, but higher amounts might increase membrane pore blockage and reduce permeability.

3) There was a negative effect of increasing the pressure on Cu removal. Higher pressures slightly reduced Cu removal efficiency, likely due to membrane compaction and reduced adsorption. The confidence intervals for the pressure were relatively narrow, indicating consistent experimental results. Increased operating pressure led to increased water flux, consistent with Darcy's law for membrane permeation.

Figure 7a, b illustrate contour plots representing the percentage of copper removal and permeate flux as functions of polymer concentration and operating pressure. The contour lines delineate the combinations of polymer concentration and pressure that produce equivalent permeate flux values. As shown in the figures, the color gradients elucidate areas of elevated or diminished permeate flux, thereby facilitating the identification of optimal operational conditions for maximizing performance. These visual indicators assist in determining the exact combination of polymer concentration and operating pressure that is capable of achieving the desired permeate flux, thereby providing critical insights for the optimization of the process.

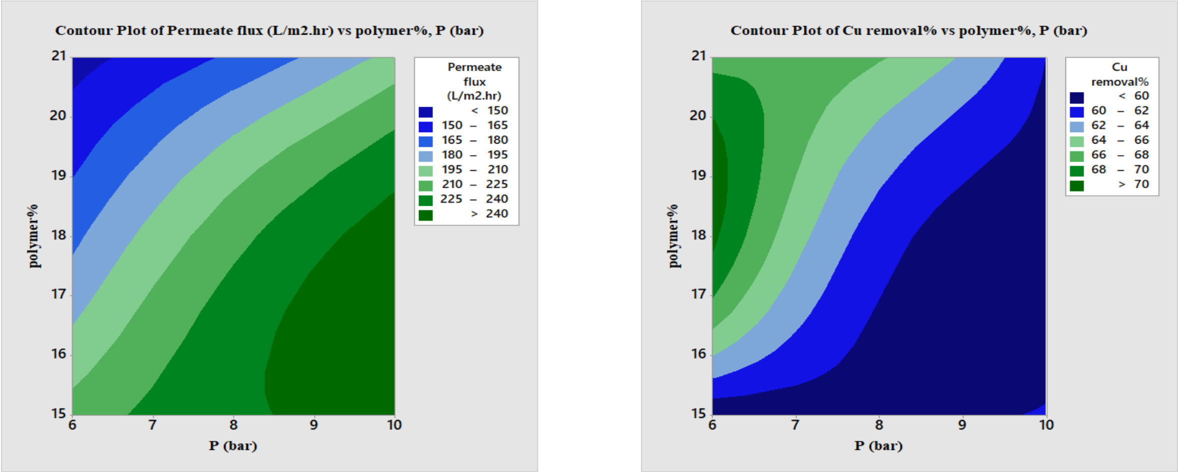

(a) (b)

Fig. 7. The contour plot for a) permeate flux and b) Cu removal% as a function of polymer concentration and operating pressure.

4. Conclusions

In the present study, GO nanoparticles were fabricated from a graphite precursor using the Hummer's method, and their surfaces were enhanced with chitosan to augment their dispersion and compatibility with the polymer matrix. Polyethersulfone membranes and mixed-matrix membranes were developed through the incorporation of these modified GO nanoparticles, and their efficacy in copper-ion separation from aqueous solutions was assessed using reverse osmosis technology. To achieve this, an experimental design was established by employing Minitab 17 software, implementing the Taguchi method with an L9 orthogonal array. The parameters influencing membrane separation, including the percentages of polymer and GO in the membrane casting solution, as well as the operating pressure during the separation process, were investigated at three distinct levels: a) 15%, 18%, and 21% for the polymer percentage; b) 0%, 0.3%, and 0.7% for the nanoparticle percentage; and c) 6, 8, and 10 bar for the operational pressure. Cross-sectional SEM images of the membranes, integrated with a statistical analysis of the experimental data using Minitab software, revealed that the three factors significantly influenced the membrane's performance in Cu removal. An ANOVA analysis was performed to determine the effects of the factors and their interactions. The p-values were assessed at a confidence level of 95% ($\alpha = 0.05$) to identify statistically significant effects. Additionally, R^2 and adjusted R^2 values were examined to assess the goodness of fit of the statistical model. The p-values of 0.011, 007, and 0.01 for the polymer concentration, GO concentration, and operating pressure indicated a statistically significant impact on the membrane performance for Cu removal with a high degree of confidence. The interval plots for Cu removal and permeate flux showed that the mean Cu removal efficiency increased with increasing polymer concentration up to 18 wt.% polymer concentration, and beyond this optimal range, the intervals slightly overlapped, indicating a diminishing effect at high concentrations. The highest flux was observed at a polymer concentration of 15 wt. %, whereas increasing the polymer concentration to 21 wt.% resulted in a decrease in flux due to an increase in the membrane structure density and a decrease in its porosity and permeability.

For the GO nanoparticle concentrations, higher GO contents led to significantly improved Cu removal but might increase membrane pore blockage and reduce permeability due to their aggregation.

The results also showed that there was a negative effect of increasing the pressure on Cu removal. Higher pressures slightly reduced Cu removal efficiency due to the reduced adsorption. The confidence intervals for the pressure were relatively narrow, indicating consistent experimental results. Increased operating pressure led to increased water flux, consistent with Darcy's law for membrane permeation.

References

[1] MacCarthy, P., Klusman, R. W., Cowling, S. W., & Rice, J. A. (1995). Water analysis. Analytical chemistry, 67(12), 525-582. https://doi.org/ 10.1021/ac00012a014

[2] Renge, V. C., Khedkar, S. V., & Pande, S. V. (2012). Removal of heavy metals from wastewater using low cost adsorbents: a review. Sci. Revs. Chem. Commun, 2(4), 580-584.

[3] Srisuwan, G., & Thongchai, P. (2002). Removal of heavy metals from electroplating wastewater by membrane. Songklanakarin J Sci Technol, 24(Suppl), 965-76.

[4] Mulungulungu, G. A., Mao, T., & Han, K. (2021). Efficient removal of high-concentration copper ions from wastewater via 2D g-C_3N_4 photocatalytic membrane filtration. Colloids and Surfaces A: Physicochemical and Engineering Aspects, 623, 126714. https://doi.org/10.1016/j.colsurfa.2021.126714

[5] Liu, N., Lu, N., Su, Y., Wang, P., & Quan, X. (2019). Fabrication of g-C3N4/Ti3C2 composite and its visible-light photocatalytic capability for ciprofloxacin degradation. Separation and Purification Technology, 211, 782-789. https://doi.org/10.1016/j.seppur.2018.10.027

[6] Ali, A., Ahmed, A.T., & Gad, A.A.M. (2016). Removal of Pb2+, Cu2+, and Cd2+ from wastewater using ceramic membrane, The 8th Int. conf. for Development and Environment in the Arab world, Assiut University Center for Environmental Studies-Egypt, 223-234.

[7] Varma V, G., & Misra, A. K. (2018). Copper contaminated wastewater–an evaluation of bioremedial options. Indoor and Built Environment, 27(1), 84-95. https://doi.org/10.1177/1420326X16669397

[8] Dermentzis, K., Davidis, A., Papadopoulou, D., Christoforidis, A., & Ouzounis, K. (2009). Copper removal from industrial wastewaters by means of electrostatic shielding driven electrodeionization. Journal of Engineering Science & Technology Review, 2(1). https://doi.org/10.25103/jestr.021.24

[9] Wang, X. S. (2009). Equilibrium and Kinetic Analysis for Cu^{2+} and Ni^{2+} adsorption onto Na-Mordenite. The Open Environmental Pollution & Toxicology Journal, 1, 107-111. https://doi.org/10.2174/1876397900901010107

[10] Taylor, A. A., Tsuji, J. S., Garry, M. R., McArdle, M. E., Goodfellow, W. L., Adams, W. J., & Menzie, C. A. (2020). Critical review of exposure and effects: implications for setting regulatory health criteria for ingested copper. Environmental management, 65, 131-159. https://doi.org/ 10.1007/s00267-019-01234-y

[11] Arbabi, M., & Golshani, N. (2016). Removal of copper ions Cu (II) from industrial wastewater: A review of removal methods. Epidemiology and Health System Journal, 3(3), 283-293.

[12] Barekat, A., & Mirzaei, M. (2017). Removal of copper (II) from aqueous solutions by sodium alginate/hydroxy apatite hydrogel modified by Zeolite. Advances in Environmental Technology, 3(4), 185-192. https://doi.org/ 10.22104/AET.2017.621

[13] Shooshtary, H., Hajiaghababaei, L., Badiei, A., Ganjali, M. R., & Mohammadi Ziarani, G. (2018). Efficient removal of Ag^+ and Cu^{2+} using imine-modified/mesoporous silica-coated magnetic nanoparticles. Advances in Environmental Technology, 4(4), 223-231. https://doi.org/10.22104/AET.2019.3324.1164

[14] Wołowicz, A., Staszak, K., & Hubicki, Z. (2022). Removal of copper (II) in the presence of sodium dodecylobenzene sulfonate from acidic effluents using adsorption on ion exchangers and micellar-enhanced ultrafiltration methods. Molecules, 27(8), 2430. https://doi.org/10.3390/molecules27082430

[15] Zou, Y. (2024). Cu^{2+}, Cd+, and Pb^{2+} ions adsorption from wastewater using polysaccharide hydrogels made of oxidized carboxymethyl cellulose and chitosan grafted with catechol groups. Iranian Polymer Journal, 33(1), 57-66. https://doi.org/10.1007/s13726-023-01234-0

[16] Kraiem, N. B., Rhimi, A., Zlaoui, K., Horchani-Naifer, K., Hafiane, A., & Ennigrou, D. J. (2024). Development of polysulfone membranes and their application for removing rare earth ions from aqueous solutions by polyvinyl alcohol-enhanced ultrafiltration. Iranian Polymer Journal, 33(10), 1481-1491. https://doi.org/10.1007/s13726-024-01325-6

[17] Xiong, X., Wang, C., Wang, R., & Duan, Y. (2024). Modification of polyvinylidene fluoride through homogeneous reaction for

preparation of hydrophilic membrane. Iranian Polymer Journal, 33(7), 901-914. https://doi.org/10.1007/s13726-024-01284-y

[18] Fallahnejad, Z., Bakeri, G., & Fauzi Ismail, A. (2024). Internally functionalized MnO2 nanotubes in modification of thin-film nanocomposite membranes for water and wastewater treatment. Iranian Polymer Journal, 33(4), 493-509. https://doi.org/10.1007/s13726-023-01264-8

[19] Quist-Jensen, C. A., Macedonio, F., & Drioli, E. (2015). Membrane technology for water production in agriculture: Desalination and wastewater reuse. Desalination, 364, 17-32. https://doi.org/10.1016/j.desal.2015.03.001

[20] Singh, R., & Hankins, N. (Eds.). (2016). Emerging membrane technology for sustainable water treatment. Elsevier.

[21] Zunita, M., Irawanti, R., Koesmawati, T. A., Lugito, G., & Wentena, I. G. (2020). Graphene oxide (Go) membrane in removing heavy metals from wastewater: a review. Chemical Engineering Transactions, 82, 415-420. https://doi.org/10.3303/CET2082070

[22] Abdullah, W. N. A. S., Tiandee, S., Lau, W., Aziz, F., & Ismail, A. F. (2020). Potential use of nanofiltration like-forward osmosis membranes for copper ion removal. Chinese Journal of Chemical Engineering, 28(2), 420-428. https://doi.org/10.1016/j.cjche.2019.05.016

[23] Mondal, M., Dutta, M., & De, S. (2017). A novel ultrafiltration grade nickel iron oxide doped hollow fiber mixed matrix membrane: Spinning, characterization and application in heavy metal removal. Separation and Purification Technology, 188, 155-166. https://doi.org/10.1016/j.seppur.2017.07.013

[24] Abd Hamid, S., Shahadat, M., Ballinger, B., Azha, S. F., Ismail, S., Ali, S. W., & Ahammad, S. Z. (2020). Role of clay-based membrane for removal of copper from aqueous solution. Journal of Saudi Chemical Society, 24(10), 785-798. https://doi.org/10.1016/j.jscs.2020.08.007

[25] Qdais, H. A., & Moussa, H. (2004). Removal of heavy metals from wastewater by membrane processes: a comparative study. Desalination, 164(2), 105-110. https://doi.org/10.1016/S0011-9164(04)00169-9

[26] Ncib, S., Chibani, A., Barhoumi, A., Larchet, C., Dammak, L., Elaloui, E., & Bouguerra, W. (2023). Separation of copper and nickel from synthetic wastewater by polymer inclusion membrane containing di (2-ethylhexyl) phosphoric acid. Polymer Bulletin, 80(11), 12177-12192. https://doi.org/10.1007/s00289-022-04634-z

[27] Hasan, A. A., & Hassoon, A. F. (2021, September). Removal of Copper ion (CU^{2+}) from Dairy wastewater by using Membrane Distillation (MD). In 2021 4th International Iraqi Conference on Engineering Technology and Their Applications (IICETA) (pp. 190-194). IEEE. https://doi.org/10.1109/IICETA51758.2021.9717714

[28] Nawaz, R., Ali, K., & Khan, M. (2016). Extraction of copper from wastewater through supported liquid membrane using tri-ethanolamine as a carrier. Desalination and Water Treatment, 57(46), 21827-21841. https://doi.org/10.1080/19443994.2015.1128986

[29] Yang, Q., & Kocherginsky, N. M. (2007). Copper removal from ammoniacal wastewater through a hollow fiber supported liquid membrane system: modeling and experimental verification. Journal of Membrane Science, 297(1-2), 121-129. https://doi.org/10.1016/j.memsci.2007.03.036

[30] Ncib, S., Barhoumi, A., Bouguerra, W., Larchet, C., Dammak, L., Hamrouni, B., & Elaloui, E. (2020). Copper (II) removal from synthetic wastewater solutions using supported liquid membrane and polymer inclusion membrane. Journal of Environmental Engineering, 146(2), 04019113. https://doi.org/10.1061/(ASCE)EE.1943-7870.0001643

[31] Akale, S., & Shaikh, I. N. (2024). Mixed-matrix membrane designed with water channels and sieving effect for effective removal of heavy metals. Environmental Nanotechnology, Monitoring & Management, 22, 100985. https://doi.org/ 10.1016/j.enmm.2024.100985

[32] Khodabakhshi, M. R., & Goodarzi, V. (2021). Preparing and analysis an innovative membrane based on polyethersulfone

/sulfonated polyethersulfone/organically modified nanoclay: Ability to heavy metal removal. Materials Today Communications, 26, 101957. https://doi.org/10.1016/j.mtcomm.2020.101957

[33] Nasr, M., Alfryyan, N., Ali, S. S., Abd El-Salam, H. M., & Shaban, M. (2022). Preparation, characterization, and performance of PES/GO woven mixed matrix nanocomposite forward osmosis membrane for water desalination. RSC advances, 12(39), 25654-25668. https://doi.org/10.1039/D2RA03832C

[34] Vatanpour, V., Madaeni, S. S., Moradian, R., Zinadini, S., & Astinchap, B. (2012). Novel antibifouling nanofiltration polyethersulfone membrane fabricated from embedding TiO2 coated multiwalled carbon nanotubes. Separation and purification technology, 90, 69-82. https://doi.org/10.1016/j.seppur.2012.02.014

[35] Wu, G., Gan, S., Cui, L., & Xu, Y. (2008). Preparation and characterization of PES/TiO_2 composite membranes. Applied Surface Science, 254(21), 7080-7086. https://doi.org/ 10.1016/j.apsusc.2008.05.221

[36] Wang, Z., Yu, H., Xia, J., Zhang, F., Li, F., Xia, Y., & Li, Y. (2012). Novel GO-blended PVDF ultrafiltration membranes. Desalination, 299, 50-54. https://doi.org/10.1016/j.desal.2012.05.015

[37] Zhao, C., Xu, X., Chen, J., & Yang, F. (2013). Effect of graphene oxide concentration on the morphologies and antifouling properties of PVDF ultrafiltration membranes. Journal of Environmental Chemical Engineering, 1(3), 349-354. https://doi.org/10.1016/j.jece.2013.05.014

[38] Peng, W., Li, H., Liu, Y., & Song, S. (2017). A review on heavy metal ions adsorption from water by graphene oxide and its composites. Journal of Molecular Liquids, 230, 496-504. https://doi.org/10.1016/j.molliq.2017.01.064

[39] Zhang, C. Z., Chen, B., Bai, Y., & Xie, J. (2018). A new functionalized reduced graphene oxide adsorbent for removing heavy metal ions in water via coordination and ion exchange. Separation Science and Technology, 53(18), 2896-2905. https://doi.org/10.1080/01496395.2018.1497655

[40] Allahbakhsh, A., Sharif, F., Mazinani, S., & Kalaee, M. R. (2014). Synthesis and characterization of graphene oxide in suspension and powder forms by chemical exfoliation method. https://doi.org/10.7508/ijnd.2014.01.002

[41] Graphene Oxide Synthesis by using Graphite, Sulphuric Acid, Potassium Permanganate and Hydrogen Peroxide via Modified Hummer's Method - InstaNANO. https://instanano.com/all/nanomaterial-synthesis/carbon/graphene-oxide-1/ (accessed December 1st, 2024).

[42] Junaidi, N. F. D., Khalil, N. A., Jahari, A. F., Shaari, N. Z. K., Shahruddin, M. Z., Alias, N. H., & Othman, N. H. (2018, May). Effect of graphene oxide (GO) on the surface morphology & hydrophilicity of polyethersulfone (PES). In IOP Conference Series: Materials Science and Engineering (Vol. 358, p. 012047). IOP Publishing. https://doi.org/10.1088/1757-899X/358/1/012047

[43] Trip, A. (1991). Taguchi methods for quality engineering. Kwantitatieve Methoden, 37, 119-135.

[44] Unal, R., & Dean, E. B. (1990). Taguchi approach to design optimization for quality and cost: an overview. In 1991 Annual conference of the international society of parametric analysts

How to cite this paper:

Khonsha, I. & salehi, K. (2025). Investigating Cu removal from wastewater using polyethersulfone-graphene oxide nanoparticles functionalized with chitosan membrane. Advances in Environmental Technology, 11(3), 329-340. DOI: 10.22104/aet.2025.7217.1987